Magnetic Resonance Studies of Wood Log-Drying Processes

Clevan Lamason Bryce MacMillan Bruce Balcom
Brigitte Leblon Zarin Pirouz

Abstract

Spatially resolved measurements of moisture content (MC) in black spruce (*Picea mariana* Mill.) logs were undertaken by unilateral magnetic resonance (UMR) and magnetic resonance imaging (MRI). The goal of this study was to understand drying behaviors of the different regions in black spruce wood logs. Results indicate that water is lost from the entire length of the log as drying progresses. Diffusive drying from both sapwood and heartwood was observed at the log ends. The most significant drying in the log interior was through the bark. The magnetic resonance signal has an amplitude that depends on water content and a lifetime that depends on the water environment, namely, cell wall or cell lumen. The UMR measurement distinguished signal from cell wall and lumen water. The MRI measurement spatially resolved, in 3D, total water content in the wood. This was important in order to differentiate the water content and drying behavior in sapwood and heartwood. The MC in the black spruce sapwood was significantly higher than the MC in the heartwood. The water content in the cell wall does not change significantly until lumen water is depleted.

Wood is a naturally occurring composite material that is hygroscopic and anisotropic with properties that are deeply influenced by the presence of water. Measurements of moisture content (MC) of wood are therefore of considerable importance. Like most natural porous materials, wood undergoes drying from its natural state to end use state. Drying processes involve the removal of moisture from the material through a variety of mechanisms, such as capillary flow and diffusion. These processes are of critical importance for wood that must be dried from its green MC prior to use as a fuel or as a construction material (Forest Products Laboratory [FPL] 2010).

The pores in wood can be filled with air or water-vapor but may also be partially or fully filled with liquid water. Water in wood exists in two different environments: (1) in the cell wall as cell wall water and (2) as lumen water in the cell lumens and other void spaces (Siau 1971, Panshin and de Zeeuw 1980, FPL 2010). The maximum water content in the cell wall is termed the fiber saturation point (FSP) and occurs around 30 percent MC for most species (Skaar 1988). The FSP is a critical parameter because most properties of wood are altered by changes in MC below the FSP.

Capillary forces determine the movement of lumen water. As wood dries, evaporation of water from the surface sets up capillary forces that exert a pull on the lumen water in zones beneath the surface (Panshin and de Zeeuw 1980, Skaar 1988). When there is no longer any lumen water in the wood, capillary forces are no longer of importance. As cell wall water is removed by diffusion, the wood shrinks. A number of physical and mechanical properties of wood are independent of MC at MCs higher than the FSP, but these properties are found to change at lower MCs as the cell wall water is removed (Siau 1971, FPL 2010).

Drying of materials is often studied by handheld moisture meters that measure the water content by indirect methods, relying on the fact that the electrical properties of the material are dependent on the water content. However, these instruments are not able to monitor the whole drying process because they are limited in effective MC range, they are point measurements, and they are in some cases intrusive. Recent developments in magnetic resonance (MR) permit monitoring the local MC (Lamason et al. 2014) with a more direct and nonintrusive approach.

Several MR and magnetic resonance imaging (MRI) studies on wood have been reported in the literature. Conventional MR and MRI techniques were used to study

The authors are, respectively, PhD Candidate, Faculty of Forestry and Environ. Manag. and MRI Research Centre, Univ. of New Brunswick, Fredericton, New Brunswick, Canada (clamason@unb.ca); Research Scientist and Professor, MRI Research Centre, Dept. of Physics, Univ. of New Brunswick, Fredericton, New Brunswick, Canada (bryce@unb.ca, bjb@unb.ca [corresponding author]); Professor, Faculty of Forestry and Environ. Manag., Univ. of New Brunswick, Fredericton, New Brunswick, Canada (bleblon@unb.ca); and Senior Research Scientist, FPInnovations, Vancouver, British Columbia, Canada (zarin.pirouz@fpinnovations.ca). This paper was received for publication in July 2016. Article no. 16-00037.

Forest Prod. J. 67(3/4):266–274.
doi:10.13073/FPJ-D-16-00037

wood anatomy and structure (Hall et al. 1986, Wang and Chang 1986, Flibotte et al. 1990), wood decay (Flibotte et al. 1990), and wood preservation (Meder et al. 1999). With respect to MC estimation, MR–MRI techniques have been used to estimate MC in wood pellets (Nyström and Dahlquist 2004) and in wood drying (Hall et al. 1986; Menon et al. 1989; Quick et al. 1990; Araujo et al. 1992; Hartley et al. 1993; Hameury and Sterley 2006; Almeida et al. 2007; Stenstrom et al. 2009; Passarini et al. 2014, 2015). Most of these studies consider relatively wet wood because conventional MRI techniques are not quantitative at low MCs.

Portable unilateral magnetic resonance (UMR) is a promising new development in MR. Numerous studies and magnet designs have been presented in the literature. Blümich et al. (2005, 2008) have recently reviewed single-sided MR. UMR may be used in many different measurement problems. In food and agriculture research, Veliyulin et al. (2008) used UMR for rapid and nondestructive determination of fat content in dairy products. Other applications include biomedicine, polymers, cultural heritage, porous media, and building materials (Blümich et al. 2008).

Lamason et al. (2015) used UMR to study water states and water content of black spruce (*Picea mariana* Mill.) and aspen (*Populus tremuloides* Michx.). They found a biexponential decay of the time-domain MR measurements that was attributed to the cell wall water (short lifetime signal) and cell lumen water (long lifetime signal).

In the current work, a portable UMR sensor and MRI measurement techniques were utilized to study drying behavior during air-drying of black spruce (*P. mariana* Mill.) logs. Results from UMR were compared with 3D centric scan single-point ramped imaging with T_1 enhancement (SPRITE) MRI measurements. The SPRITE MRI technique can spatially resolve, in 3D, total water content in wood. A detailed description of centric scan SPRITE has been published in Halse et al. (2003). Readers are referred to Lamason et al. (2014) for relevant discussions of SPRITE MRI and water content measurements in wood materials.

Several log drying models have been presented in the literature. Droessler et al. (1986) investigated the influence of weather conditions on drying rates. They found that the rate of weight loss in freshly cut, piled wood logs was largely constant but was influenced by environmental conditions, such as average daily high temperature, average high humidity, and total rainfall in the days immediately preceding measurement. Fauchon et al. (2000) developed a model to estimate the drying rate of logs during storage. Their model takes into account the initial MC and relative humidity of ambient air. Simpson and Wang (2004) developed a model to predict air-drying times of small-diameter ponderosa pine and Douglas-fir logs. Schultz et al. (1997) developed a more advanced model and reported that species, days in storage, and log diameter had the greatest effects on drying behavior, while the effect of drying through log ends on overall log moisture loss was relatively minor. Schultz et al. (1997) argued that the radial drying through the bark dominates because (1) radial distances from the log center to the bark provided a much shorter path for water evaporation than longitudinal travel and (2) the surface area for radial moisture paths was many times greater than the surface area of log ends. Radial gradients in MC were observed by Schultz et al. (1997) through coarse sectioning and drying. Defo and Brunette (2006) developed a log-drying model based on the concept of water potential. They presented simulations of the effect of bark loss on drying.

Simple mass measurements were used by the authors of the above models. They assumed the wood log is a homogenous cylinder with a single type of water. These assumptions automatically preclude a realistic model. Wood consists of sapwood and heartwood that will have different drying behaviors, and water in wood exists in two different environments (cell wall and cell lumen) with different physical behaviors. In addition, the majority of traditional measurements have coarse spatial resolution and cannot observe moisture gradients. While the above assumptions may be reasonable to a first approximation, they preclude a more rigorous examination of mechanisms and thereby the assembly of high-quality drying models. Measurements that permit differentiation between sapwood and heartwood and that distinguish cell wall and cell lumen water while measuring local MC and MC gradients will be invaluable to evaluate drying mechanisms and to help assemble future drying models.

This study was aimed at understanding the behavior of water in black spruce wood logs during drying. The UMR and MRI measurements were applied to spatially resolve water content in a black spruce (*P. mariana* Mill.) log. These measurements allowed quantification of water content in sapwood and heartwood regions and, in the case of UMR measurements, differentiated cell wall and cell lumen water. These experimental data will help improve existing wood drying models for better and more accurate predictions of water content.

Materials and Methods

A freshly cut black spruce butt log approximately 10.8 to 11.4 cm in diameter and 1.8 m in length was used for this study. The log had approximately 80 growth rings at cross section. The fresh weight of the log was 15.8 kg. Two 2.5-cm-thick disks, one from each end, were cut for gravimetric MC measurements. Polyurethane reference markers on the log surface were applied for MRI image registration. Markers were fixed on the bark in a straight line for the full length of the log. Adjacent markers were spaced 3.8 cm apart. The log was maintained in an environmental chamber set at 20°C and 65 percent relative humidity. UMR and SPRITE MRI measurements were undertaken during air-drying over a 4-month period. All measurements were undertaken in the laboratory with the log maintained in an environmental chamber for the entire study. The log ends were wrapped with cellophane during UMR and MRI measurements to prevent moisture loss during measurement.

The UMR measurements were performed with a three-magnet array UMR device developed at the University of New Brunswick MRI Centre. The device is lightweight, features open access, and is portable (Marble et al. 2007). It produces a uniform magnetic field of 0.1 Tesla, located approximately 1.3 cm measured from the top surface of the magnet. The radio frequency coil, in combination with the static field topology, gives a sensitive spot for MR measurement of approximately 1 cm^3. This permits the signal to be measured within a finite volume inside the sample at a fixed depth within the log. Figure 1 shows a schematic diagram of a cross section of wood log and UMR showing the sensitive spot displaced from the surface of the magnet with respect to the different regions of the wood. As

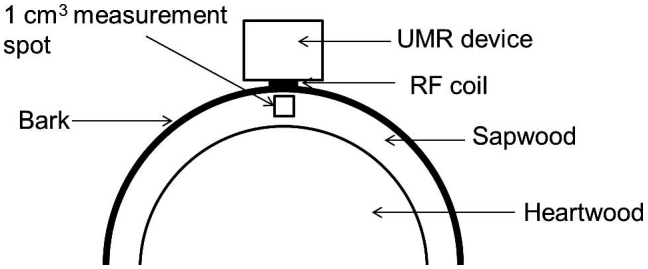

Figure 1.—Schematic diagram of the wood log and unilateral magnetic resonance (UMR) device in cross section showing the sensitive spot with respect to the different regions of the wood. The measurement spot is solely in the sapwood. The diagram is drawn to scale. RF = radio frequency.

indicated in the figure, the sensitive spot is located in the sapwood region, below the bark.

The MR frequency in the sensitive spot was 4.46 MHz. The UMR measurements were performed with a Bruker Minispec mq10 NMR Analyzer (Rheinstetten, Germany) with a Carr Purcell Meiboom Gill (CPMG) measurement that measures the transverse relaxation time T_2 and signal amplitude. The initial MR signal amplitude is proportional to MC. CPMG measurement parameters were 90° pulse length = 10 μs, echo time = 160 μs, scans = 512, and number of echoes = 1,024. The acquisition time was approximately 10 minutes for each UMR measurement.

The UMR measurements were undertaken for sapwood along the length of the log, through the bark, with 7.6 cm spacing between measurement spots. The CPMG decays were analyzed using a biexponential fitting, performed with a least-squares regression in SigmaPlot (Systat Software Inc.).

The CPMG decay constant is the T_2 relaxation time. A biexponential fitting permitted determination of the relative water content in different environments (cell wall and cell lumen), based on the lifetime of the MR signal. The short lifetime signal component is related to the cell wall water, while the long lifetime signal component is related to the lumen water (Lamason et al. 2015). The sum of the two signal populations were then converted into MCs by using a reference sample of known MC. The reference sample had 30 percent MC and was fabricated from a mix of H_2O, deuterium oxide (D_2O), and copper sulfate.

The CPMG measurements employed by the UMR allowed quantification of both short and long lifetime signal components. The UMR measurements were compared with 3D SPRITE MRI images acquired using a Nalorac (Nalorac Cryogenics Inc., Martinez, California) 2.4-Tesla horizontal bore superconducting magnet. The ambient temperature was 12°C. SPRITE 3D imaging parameters were number of scans = 8, time between gradient steps = 2 ms, maximum T_p in an eight-point acquisition = 264 μs, time between interleaves = 500 ms, matrix size = 64 by 64 by 64, maximum gradient = 2.5 G/cm, and field of view = 13 cm. The RF probe was a bird cage, 13 cm in diameter. The RF flip angle was 25°. The nominal image resolution was 0.2 cm per pixel, and the total acquisition time was 20 minutes for each image.

The SPRITE MRI measurement was 3D encompassing the entire wood cross-sectional volume, while the UMR measurement was limited to a relatively large sensitive volume in the near-surface sapwood, below the bark. The UMR measurement spot is translated longitudinally from one end of the log to the other.

Results and Discussion

The gravimetric MC of the fresh log was 63 percent based on the average of two 2.5-cm-thick wood disks cut from the log, one from each end. The bark thickness was approximately 2 mm. The sapwood thickness was approximately 1.5 cm.

The UMR CPMG measurement of a freshly cut log revealed an MR signal that decayed biexponentially, as shown in Figure 2. The short lifetime signal component from a freshly cut black spruce sapwood is associated with the water in the cell walls, while the long lifetime signal component is associated with the lumen water (Riggin et al. 1979; Menon et al. 1987, 1989; Araujo et al. 1992; Lamason et al. 2015). The initial MR signal intensity is proportional to the overall quantity of water. The total MC is equal to the sum of the signal from the two water environments. Signal intensity decreased as the sample dried. No signal was detected from the long lifetime signal component at an MC lower than 18 percent (Fig. 2b). At initial MC, the ratio of cell wall to lumen water in the sapwood, along the length of the log, ranged from 1:3.0 to 1:3.4. This ratio was computed based on the y-intercepts of the short and long lifetime signal components of the CPMG decay. This is consistent with the conceptual definition of FSP. At an MC of 132 percent, the lumen water quantity is greater by a factor of 3.4 compared with the cell wall water, assuming an FSP of around 30 percent MC. At initial conditions, the observed T_2 values of short (cell wall) and long (lumen) lifetime signal components ranged from 1 to 8 ms and 84 to 96 ms, respectively.

The observed relaxation rate ($1/T_2$) from the water in the lumen (free water) is the weighted average rate of both the surface and the bulk water (Menon et al. 1987, Wong 1999). Typically, there is more bulk water in the cell volume than surface water when the wood is green, but the surface relaxation rate is much greater than the bulk relaxation rate. As lumen water is removed, the average T_2 of the long lifetime signal component decreases because the surface water contribution to T_2 increases in significance.

A biexponential fitting of the CPMG decay gave a satisfactory fit to the experimental decay. This was supported by a high R^2, low standard error of estimate, and analysis of variance results. Previous work on spin–spin relaxation rates in wood suggested that MR measurements could differentiate lumen water in earlywood and latewood owing to different cell cavity sizes. However, three discrete exponentials were not observed in the current work. Menon et al. (1987, 1989) assigned earlywood and latewood lumen water (different cell cavity sizes) to the longer two of three observed time constants in their work. In the current work, we were unable to resolve separately earlywood and latewood contributions. We assume that the long lifetime T_2 observed and reported is an average of the cell lumen water in earlywood and latewood.

The total MC in sapwood as a function of position along the length of the log, through the bark, is presented in Figure 3. As indicated in Figure 3, there were slight changes to MC along the length from Day 1 to Week 1. However, a significant drop in the overall MC was observed throughout the length of the log after 1, 2, and 4 months of air-drying. The near end surfaces of the log were below 40 percent MC

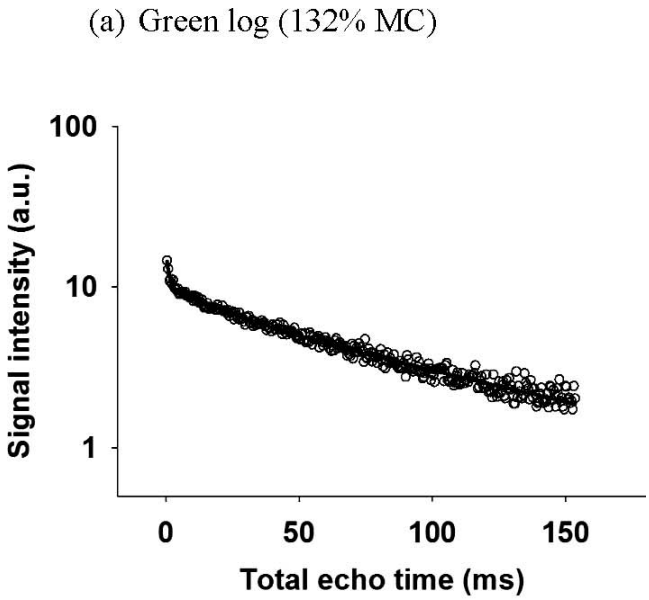

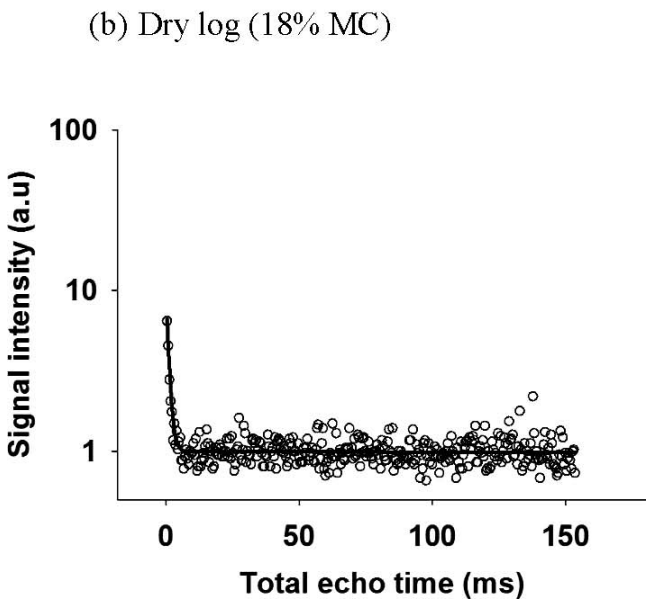

Figure 2.—Biexponential Carr Purcell Meiboom Gill (CPMG) decay plots of signal intensity of freshly cut (a) and 2-month air-dried (b) black spruce sapwood using the 4.46-MHz unilateral magnet instrument. Measurements were undertaken near the end of the log through the bark. The solid line is the best-fit biexponential decay of the short (cell wall) and long (lumen) lifetime signal components. In this measurement, the ratio of lumen to cell wall water was 3.4 in the freshly cut sample (a). Only the short lifetime signal component was observed from the sample at 18 percent moisture content (b).

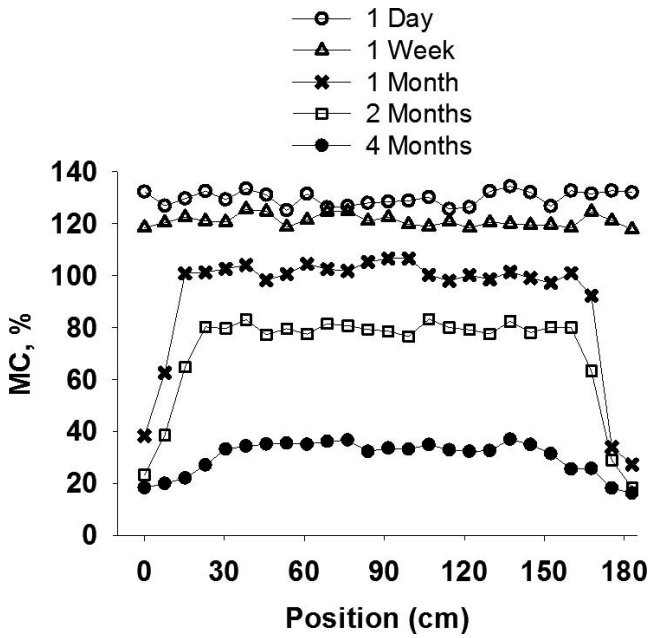

Figure 3.—Measured total moisture content (MC) in sapwood as a function of positon along the full length of the log through the bark. A unilateral magnet utilizing Carr Purcell Meiboom Gill (CPMG) measurements was used. The unilateral magnetic resonance measurements allowed quantification of both short and long T_2 water lifetime components. The sample ends were below 30 percent MC after 2 months of air-drying.

after 1 month of air-drying. Overall, the signal decreases from Day 1 to 4 months; however, for each drying time, the signal is spatially uniform displaced from the ends. This uniform drop in signal along the length in the interior of the sample is an indication of radial drying through the bark as explained below. This radial drying mechanism provided greater MC loss than capillary drying in the longitudinal direction. This is consistent with the findings of Schultz et al. (1997), who reasoned that the radial distance from the log center to the bark provided a much shorter path for water evaporation than longitudinal travel. The end surfaces dried because of capillary and diffusive moisture losses through the exposed end. After 4 months, the MC of all measurement spots in the sapwood was below 40 percent MC.

Because the MR signal intensity is proportional to the MC, the signal associated with the different relaxation times reflects the amount of water in the different states (Lamason et al. 2015). The change in the signal amplitude of lumen and cell wall water in the sapwood as determined by the UMR instrument is presented in Figure 4.

No signal was detected from the sapwood lumen water at both ends of the log after 2 months of air-drying (Fig. 4d). Initially, the MC of sapwood along the length of the log ranged from 125 to 135 percent. The cell wall water signal intensity did not change significantly above 30 percent MC. This result is in agreement with Zhang et al. (2013) and Lamason et al. (2015), who reported that cell wall water does not change significantly above 40 percent MC. No signal from lumen water was detected at or below 20 percent MC. The cell wall MC did not change significantly in the early stages of drying. After 1 month of drying, the cell wall MC was below FSP at both ends of the log. After 4 months, minimal lumen water was observed in all the measurement spots along the full length of the log.

At initial conditions, the T_2 value of cell wall water is constant (not shown in Fig. 4). Lumen water T_2 ranged from 84 to 96 ms at initial conditions; however, as lumen water is removed during drying, the corresponding T_2 decreases. The T_2 decreases because the surface-to-volume ratio changes as water fills only part of the cell volume. The T_2 of a

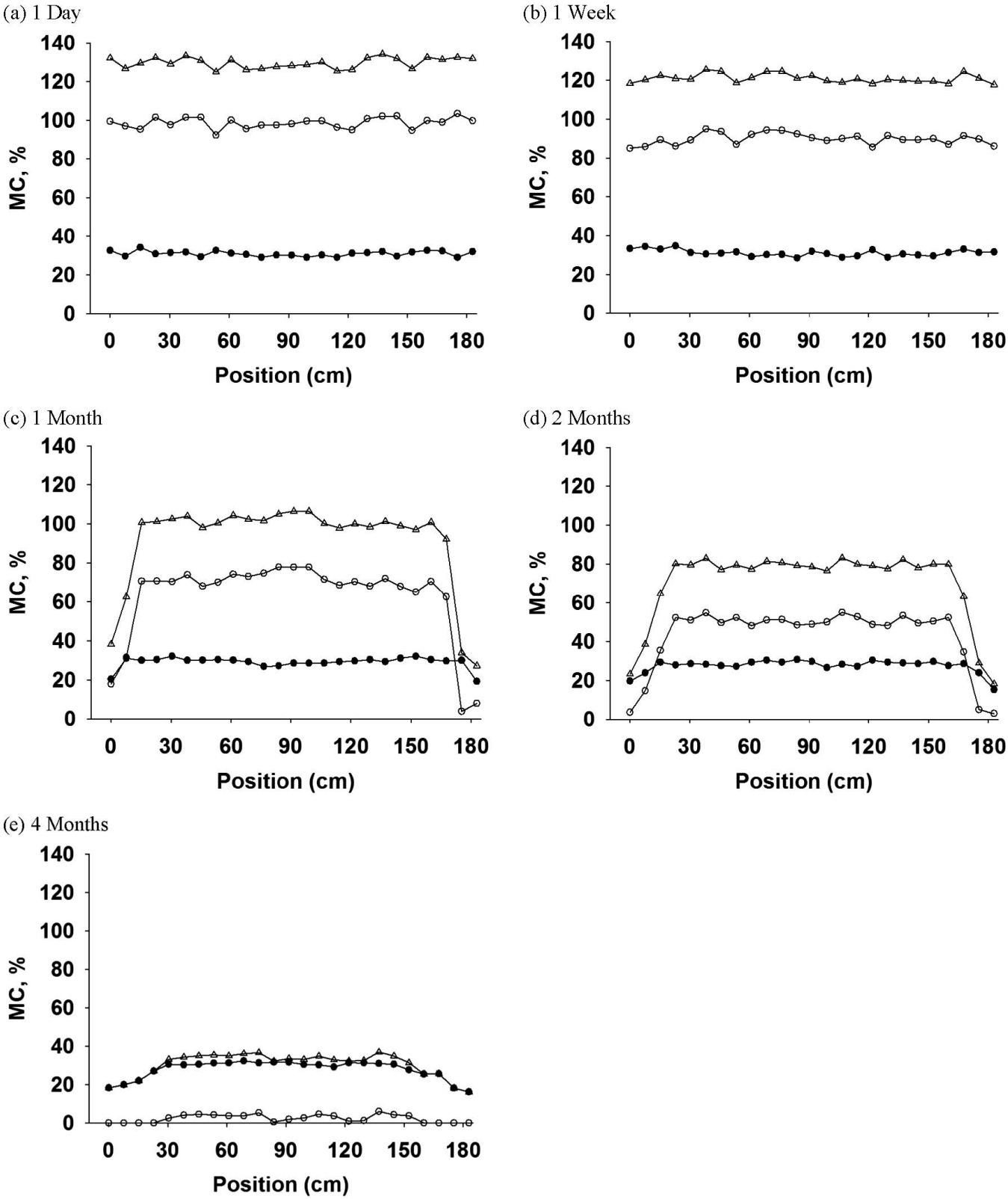

Figure 4.—Total water (Δ) in black spruce sapwood as determined by magnetic resonance as a function of sample length. Total water is cell wall water plus lumen water. Signal from cell wall water (●) does not change with moisture content (MC) above 30 percent. No signal is detected from the lumen water (○) at both ends of the log after 2 months of air-drying. Air-drying durations: (a) 1 day, (b) 1 week, (c) 1 month, (d) 2 months, and (e) 4 months. No significant change in MC in the cell wall was observed until the MC was below the fiber saturation point.

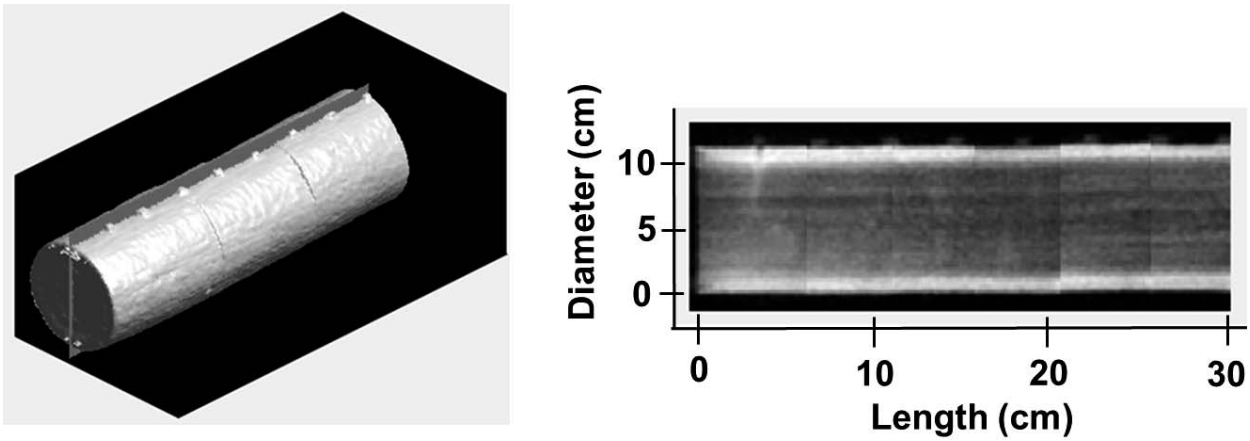

Figure 5.—Single-point ramped imaging with T_1 enhancement magnetic resonance imaging (SPRITE MRI) composite images of a black spruce log in 3D (left) and a 2D slice extracted from the 3D image on the left as indicated by the slice plane. These are not images of the entire log sample. These joined images represent 30.5 cm of the log length, starting at one end. Measurements were taken at the start of the drying study. In these images, the small markers placed at intervals along the log are visible. These markers were used for image registration because the total length of the sample is longer than the image field of view. The sapwood region has higher signal intensity compared with the heartwood region, indicating that the sapwood has high moisture content.

particular cell cavity size will decrease as water is removed. A partially filled cavity will have a shorter T_2 than a fully saturated cavity.

Figure 5 shows SPRITE MRI images of a black spruce log in 3D (left) and as a 2D slice extracted from the 3D image as indicated by the slice plane. These are not images of the whole sample, but rather a composite of many individual images. The composite image in Figure 5 shows a 30.5-cm length of the log, starting at one end. These measurements were taken at the start of the drying study, which immediately followed harvesting of the tree. The log was preserved during preparation and transport from the field to the laboratory. In these images, the small markers placed at intervals along the log are visible. These markers were used for image registration because the total length of the log was greater than the image field of view. The sapwood region has higher signal intensity compared with the heartwood region indicating that the sapwood has higher MC than the heartwood. The 2D image slice reveals a knot directly below the leftmost marker on the top. Note the presence of discontinuities in the 2D slices that were due to difficulty in splicing discrete images.

MC in sapwood (Fig. 6a) and heartwood (Fig. 6b) as a function of position along the length of the log are given in Figure 6. Positions 0 and 91 cm correspond to the end and midpoint along the length, respectively. These 1D profiles were averages of three profiles along the sapwood and were extracted from the 3D SPRITE MRI composite images. A decrease in MC was observed with increased drying duration. Diffusive drying was observed at the end of the sample and is immediately apparent on Day 1. Both Figure 3 and Figure 6a reveal uniform water content and uniform water loss, except at the ends. For sapwood (Fig. 6a), the diffusive drying front has penetrated approximately 9 cm from the end after 1 month of air-drying. For heartwood (Fig. 6b), the diffusive drying front penetrated from the end within 1 week of air-drying. The MC of heartwood in the interior is constant until after 2 months of air-drying. Although diffusive end drying was immediately apparent at early drying times, the more significant loss of MC was observed in the radial direction of the log (as discussed below).

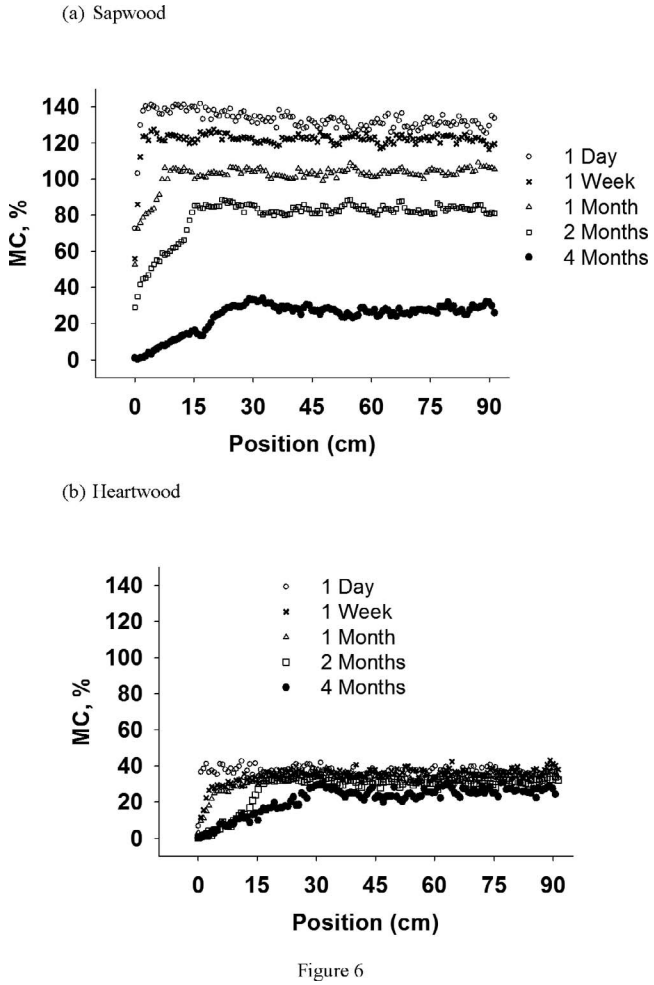

Figure 6

Figure 6.—Moisture content (MC) in sapwood (a) and heartwood (b) as a function of position along the length of the log. Positions 0 and 91 cm correspond to the end and midpoint along the length, respectively. These 1D profiles were extracted from the 3D single-point ramped imaging with T_1 enhancement magnetic resonance imaging (SPRITE MRI) images. A decrease in MC was observed with increased drying duration. Diffusive drying was observed at the end of the sample.

Figure 7 shows SPRITE MRI images of the black spruce log in the transverse direction (left) and radial profiles (right) extracted from the image at the central vertical line of the image, for three positions along the length of the log. These data were taken after 1 month of air-drying. The sapwood region has higher signal intensity compared with the heartwood region, indicating that the sapwood has higher MC than heartwood. A drying front is observed near the end of the log. The MC in the sapwood and heartwood regions at the end of the log is less than the MC in regions displaced from the end. Heterogeneity in MC in the heartwood region is apparent from variation in image intensity in the 2D slices as well as in the radial profiles. The bottom MRI image shows the presence of knots in the transverse plane. The end and heartwood portion of the knots appeared to have drier regions compared with the neighboring sapwood.

Radial drying through the bark was observed during the course of the drying study. Figure 8 gives the MC profiles in the vertical direction corresponding to the central transverse plane of the log (refer to Fig. 7). The location of the UMR sensitive spot measurement is noted in the figure. It is located in the sapwood below the bark. The UMR measurement averages the MC in the sensitive spot. This figure shows that the MC varies radially within the region of sample measured by UMR. The UMR measurements provide an average signal from a gradient of MC as revealed in the MRI SPRITE measurement. MC decreases

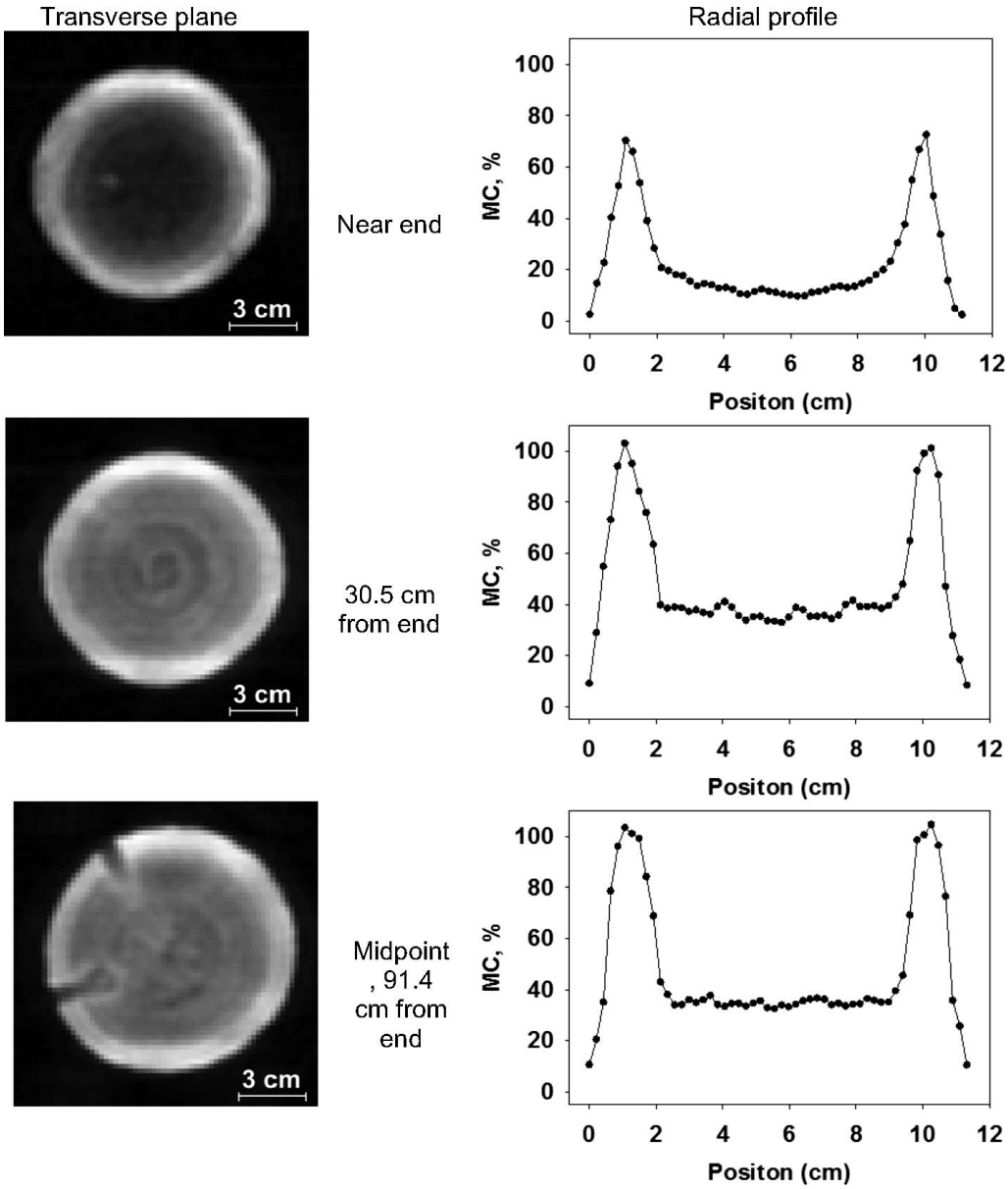

Figure 7.—Single-point ramped imaging with T_1 enhancement magnetic resonance imaging (SPRITE MRI) images of black spruce log in the transverse plane (left) and radial profiles (right) extracted vertically at the center of the composite image as a function of position along the length of the log. These data were taken after 1 month of air-drying. The sapwood region has higher signal intensity compared with the heartwood region, indicating that the sapwood has high moisture content (MC). A drying front was observed near the end of the log. The MC in the sapwood and heartwood regions near the end was less than the MC in regions displaced from the end.

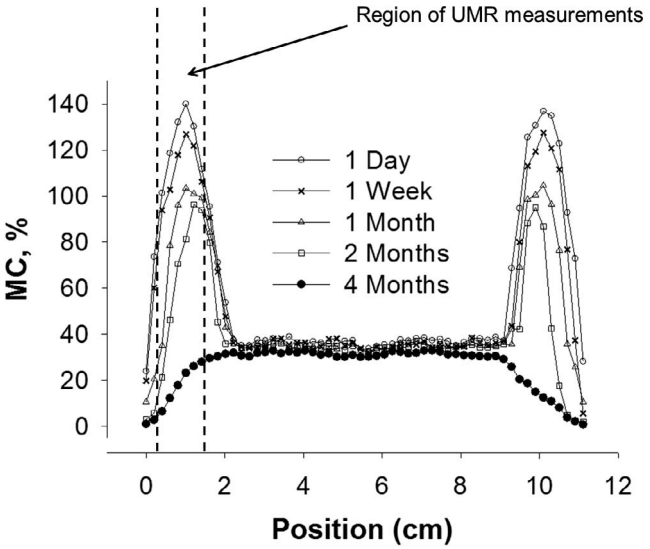

Figure 8.—Moisture content (MC) in the vertical direction, corresponding to the central transverse plane of the log at the midpoint along its length. A moisture gradient through the sapwood in the radial direction is observed owing to diffusive drying through the bark. MC decreases with air-drying duration. In heartwood, no significant change in MC was observed at early drying times; however, a drop in MC was observed after 4 months of air-drying. The position of the unilateral magnetic resonance–sensitive spot is illustrated. Data for heartwood MC, not the sapwood, was smoothed with a three-point moving average.

with air-drying duration. A moisture gradient through the sapwood in the radial direction was observed owing to diffusive drying through the bark. Anatomical features, such as rays, are responsible for the movement of water through the bark (Panshin and de Zeeuw 1980). The MC in the heartwood region, midpoint along the length of the log, is constant up to 2 months of drying. Away from the sample ends, the MC of the heartwood decreases only once the MC of the adjoining sapwood is below that of the heartwood.

Conclusions

The application of MR measurement techniques in the study of a wood log drying allowed better understanding of its drying mechanisms. Both the UMR and the SPRITE MRI results are in agreement pertaining to the observed drying behavior and MC estimation. There is evidence of diffusive end drying and radial drying through the bark. The effect of radial drying through the bark is more significant compared with the diffusive end drying even though the diffusive end drying was immediately apparent from Day 1.

The sapwood region has higher signal intensity compared with the heartwood region, indicating that the sapwood has higher MC than heartwood. Results indicate that diffusive drying occurred at the ends of the log for both sapwood and heartwood. Substantial radial drying through the bark was observed in the interior of the log. The water content in the cell wall does not change significantly until lumen water is depleted. Although this work considers a wood log as the sample, we infer that MR and MRI measurements of MC used here can be translated to other wood materials, such as lumber, timber, engineered wood products, and composites, where nondestructive and direct water content measurements is of vital significance.

The UMR and MRI measurements used allowed spatially resolved measurements of MC, which is beneficial in determining and understanding the MC gradients present in the sample. Traditional wood drying models apply mass measurements, destructive techniques, and bulk MC measurements that automatically make determination of MC gradients problematic.

In addition, we have demonstrated that the UMR and MRI measurements are powerful tools that can be used to verify existing wood drying models. Based on this study, a good drying model should include drying behaviors of cell wall and lumen water as well as drying kinetics present in sapwood and heartwood regions.

Acknowledgments

The authors wish to thank the Natural Sciences and Engineering Research Council (NSERC) of Canada for a Strategic Grant awarded to Brigitte Leblon and coworkers. Clevan Lamason thanks NSERC of Canada for a PGS D award (2012–2015). Bruce Balcom thanks the Canada Chairs program for a Research Chair in MRI of Materials (2009–2023) and NSERC for a Discovery grant. The authors thank FPInnovations for in-kind support.

Literature Cited

Almeida, G., S. Gagne, and R. E. Hernández. 2007. A NMR study of water distribution in hardwoods at several equilibrium moisture contents. *Wood Sci. Technol*. 41(4):293–307.

Araujo, C. D., A. L. MacKay, J. R. T. Hailey, K. P. Whittall, and H. Le. 1992. Proton magnetic resonance techniques for characterization of water in wood: Application to white spruce. *Wood Sci. Technol*. 26(2):101–113.

Blümich, B., F. Casanova, J. Perlo, S. Anferova, V. Anferov, K. Kremer, N. Goga, K. Kupferschlager, and M. Adams. 2005. Advances of unilateral mobile NMR in non-destructive materials testing. *Magn. Reson. Imaging* 23(2):197–201.

Blümich, B., J. Perlo, and F. Casanova. 2008. Mobile single-sided NMR. *Prog. Nucl. Magn. Reson. Spectrosc*. 52:197–269.

Defo, M. and G. Brunette. 2006. A log drying model and its application to the simulation of the impact of bark loss. *Forest Prod. J*. 56(5):71–77.

Droessler, T., J. L. Bowyer, T. Burk, E. Jamrock, and R. Antilla. 1986. Rate of weight loss in piled pulpwood. Bulletin AD-Sb-3036. Agricultural Experimental Station, University of Minnesota, St. Paul. 18 pp.

Fauchon, T., G. Chantre, and C. Deleuze. 2000. How to control the variation of the wood moisture content of logs from the stand to the wood yard? The contribution of both direct techniques of assessment and modeling. *In:* Proceedings of the 2000 TAPPI Pulping/Process and Product Quality Conference, November 5–8, 2000, Boston, Massachusetts; TAPPI Press, Atlanta. pp. 419–431.

Flibotte, S., R. S. Menon, A. L. MacKay, and J. R. T. Hailey. 1990. Proton magnetic resonance of western red cedar. *Wood Fiber Sci*. 22(4):362–376.

Forest Products Laboratory (FPL). 2010. Wood handbook—Wood as an engineering material. General Technical Report FPL-GTR-190. USDA Forest Service, Forest Products Laboratory, Madison, Wisconsin. 508 pp.

Hall, L. D., V. Rajanayagam, W. A. Stewart, and P. R. Steiner. 1986. Magnetic resonance imaging of wood. *Can. J. Forest Res*. 16(2):423–426.

Halse, M., D. J. Goodyear, B. MacMillan, P. Szomolanyi, D. Matheson, and B. J. Balcom. 2003. Centric scan *SPRITE* magnetic resonance imaging. *J. Magn. Reson*. 165(2):219–229.

Hameury, S. and M. Sterley. 2006. Magnetic resonance imaging of moisture distribution in *Pinus sylvestris* L. exposed to daily indoor relative humidity fluctuations. *Wood Mater. Sci. Eng*. 1:116–126.

Hartley, I. D., F. A. Kamke, and H. Peemoeller. 1993. Absolute moisture content determination of aspen wood below the fiber saturation point using pulsed NMR. *Holzforschung* 48(6):474–479.

Lamason, C., B. MacMillan, B. J. Balcom, B. Leblon, and Z. Pirouz. 2014. Examination of water phase transitions in black spruce by magnetic resonance and magnetic resonance imaging. *Wood Fiber Sci*. 46(4):1–14.

Lamason, C., B. MacMillan, B. J. Balcom, B. Leblon, and Z. Pirouz. 2015. Water content measurement in black spruce and aspen sapwood with bencthtop and portable magnetic resonance devices. *Wood Mater. Sci. Eng*. 10(1):86–93.

Marble, A. E., I. V. Mastikhin, B. G. Colpitts, and B. J. Balcom. 2007. A compact permanent magnet array with a remote homogenous field. *J. Magn. Reson*. 186(1):100–104.

Meder, R., R. A. Franich, and P. T. Callaghan. 1999. ^{11}B magnetic resonance imaging and MAS spectroscopy of trimethylborate-treated radiate pine wood. *Solid State Nucl. Magn. Reson*. 15(1):69–72.

Menon, R. S., A. L. Mackay, S. Flibotte, and J. R. T. Hailey. 1989. Quantitative separation of NMR images of water in wood on the basis of T_2. *J. Magn. Reson*. 82:205–210.

Menon, R. S., A. L. MacKay, J. R. T. Hailey, M. Bloom, A. E. Burgess, and J. S. Swanson. 1987. An NMR determination of the physiological water distribution in wood during drying. *J. Appl. Polym. Sci*. 33:1141–1155.

Nyström, J. and E. Dahlquist. 2004. Methods for determination of moisture content in wood chips for power plants—A review. *Fuel* 83:773–779.

Panshin, A. J. and C. de Zeeuw. 1980. Textbook of Wood Technology. 4th ed. McGraw-Hill, New York. 722 pp.

Passarini, L., C. Malveau, and R. E. Hernández. 2014. Water state study of wood structure of four hardwoods below fiber saturation point with NMR technique. *Wood Fiber Sci*. 46:480–488.

Passarini, L., C. Malveau, and R. E. Hernández. 2015. Distribution of the equilibrium moisture content in four hardwoods below fiber saturation point with magnetic resonance microimaging. *Wood Sci. Technol*. 49(6):1251–1268.

Quick, J. J., J. R. T. Hailey, and A. L. MacKay. 1990. Radial moisture profiles of cedar sapwood during drying: A proton magnetic resonance study. *Wood Fiber Sci*. 22(4):404–412.

Riggin, M. T., A. R. Sharp, R. Kaiser, and M. H. Schneider. 1979. Transverse NMR relaxation of water in wood. *J. Appl. Polym. Sci*. 23(11):3147–3154.

Schultz, E. B., T. G. Matney, and W. F. Watson. 1997. Prediction of moisture contents for sprinkled and un-sprinkled stacked roundwood over time. *In:* Proceedings of the TAPPI Pulping Conference, October 19–23, 1997, San Francisco, California; TAPPI Press, Atlanta. pp. 289–299.

Siau, J. F. 1971. Flow in Wood. Syracuse University Press, Syracuse, New York. 131 pp.

Simpson, W. T. and X. Wang. 2004. Estimating air-drying times of small diameter ponderosa pine and Douglas-fir logs. *Forest Prod. J*. 54(12):24–28.

Skaar, C. 1988. Wood-Water Relations. Springer-Verlag, New York. 283 pp.

Stenstrom, S., C. Bonazzi, and L. Foucat. 2009. Magnetic resonance imaging for determination of moisture profiles and drying curves. *In:* Modern Drying Technology. Vol. 2. Experimental Techniques. E. Tsotsas and A. S. Mujumdar (Eds.). Wiley-VCH, Weinheim, Germany. pp. 91–142.

Veliyulin, E., I. V. Mastikhin, A. E. Marble, and B. J. Balcom. 2008. Rapid determination of the fat content in packaged dairy products by unilateral NMR. *J. Sci. Food Agric*. 88:2563–2567.

Wang, P. C. and S. J. Chang. 1986. Nuclear magnetic resonance imaging of wood. *Wood Fiber Sci*. 18(2):308–314.

Wong, P. 1999. Methods in the Physics of Porous Media. Academic Press, San Diego, California.

Zhang, M., X. W. Wang, and R. Gazo. 2013. Water states in yellow poplar during drying studied by time-domain nuclear magnetic resonance. *Wood Fiber Sci*. 45(4):1–6.